

Proximity Effect in Normal Metal - High T_c Superconductor Contacts

Tomas Löfwander

Department of Physics & Astronomy, Northwestern University, Evanston, IL 60208

(Dated: October 29, 2018)

We study the proximity effect in good contacts between normal metals and high T_c ($d_{x^2-y^2}$ -wave) superconductors. We present theoretical results for the spatially dependent order parameter and local density of states, including effects of impurity scattering in the two sides, s -wave pairing interaction in the normal metal side (attractive or repulsive), as well as subdominant s -wave pairing in the superconductor side. For the [100] orientation, a real combination $d + s$ of the order parameters is always found. The spectral signatures of the proximity effect in the normal metal includes a suppression of the low-energy density of states and a finite energy peak structure. These features are mainly due to the impurity self-energies, which dominate over the effects of induced pair potentials. For the [110] orientation, for moderate transparencies, induction of a $d + is$ order parameter on the superconductor side, leads to a proximity induced is order parameter also in the normal metal. The spectral signatures of this type of proximity effect are potentially useful for probing time-reversal symmetry breaking at a [110] interface.

PACS numbers: 74.45.+c, 74.20.Rp

I. INTRODUCTION

The proximity effect refers to a broad range of phenomena related to the leakage of superconducting correlations into a normal metal in contact with a superconductor. One way of viewing the proximity effect, is to consider the decay of the electron pair wave function, or off-diagonal retarded Green's function f^R , from the superconductor side to the normal metal side, on the coherence length scale.¹

The proximity effect in a normal metal in good contact with a low- T_c superconductor has been studied for a long time^{1,2,3,4,5,6,7,8} (see also the review in Ref. 9 and references therein). On the other hand, the proximity effect in a normal metal in good contact with a high- T_c superconductor has not been considered experimentally until very recently.^{10,11}

Sharoni *et al.*¹¹ performed scanning tunneling spectroscopy on gold coated $\text{YBa}_2\text{Cu}_3\text{O}_{7-\delta}$ (YBCO), and found a (pseudo-) gap on the gold side that decayed exponentially with distance from the superconductor on a scale ~ 30 nm. Kohen *et al.*¹⁰ measured the conductance of a contact between gold and $\text{Y}_{1-x}\text{Ca}_x\text{Ba}_2\text{Cu}_3\text{O}_{7-\delta}$. The experimental results were fitted with BTK-type¹² (Blonder-Tinkham-Klapwijk) model generalized to include the $d_{x^2-y^2}$ symmetry of the order parameter,¹³ as well as a subdominant component of the order parameter of s or d_{xy} symmetry. The authors of Ref. 10 concluded from their fits that the order parameter on the superconductor side might have the time-reversal symmetry breaking (TRSB) form $d + is$. This result was rather surprising, since the contacts had predominantly [100] orientation and very high transparency, in which case TRSB is usually not expected (see e.g. Refs. 14,15 and the reviews in Refs. 16,17). Therefore, the authors speculated that maybe there is an *unusual proximity effect*, where the TRSB state is induced by the proximity effect at a good contact between a normal metal and $d_{x^2-y^2}$

superconductor with [100] orientation. The authors of Ref. 11 later speculated, based on the size of the pseudogap seen in their STM spectroscopy, that they might also have observed this type of new symmetry breaking.

Motivated by these experiments, we set out to explore the proximity effect in normal metal - high- T_c superconductor structures. We do *not* find any evidence of a new symmetry breaking proximity effect, within our model and its parameter space. But, on the other hand, we are able to qualitatively explain the pseudogap phenomenon seen in the latter experiment¹¹ in terms of a more conventional type of proximity effect where the modulation in the local density of states is due to the interplay of leaking superconducting correlations into the normal metal and impurity scattering.

II. MODEL AND METHODS

We shall describe two types of systems: first, an NIS system where a normal metal (N) is coupled to an [100] (a -axis) high- T_c superconductor (S) facet through a high-transparency tunnel barrier (I), as shown in Fig. 1. This setup roughly corresponds to the experimental situation.¹¹ We will also present results for a [110]-contact. Second, an INIS system consisting of an a -facet with a metal overlayer, shown in Fig. 2.

Our considerations will be applicable to rather general situations, but in order to match the experimental conditions we restrict the parameter space of our model. We focus on the low temperature region $T = 0.05T_c$, where T_c is the superconducting transition temperature ($T = 4.2\text{K}$ and $T_c = 90\text{K}$ in the experiment). In the S-side we include, besides the d -wave interaction, an attractive pairing interaction in the s -wave channel with a critical temperature $T_{cs} = 0.1T_c$, which is similar in magnitude to previous estimates from measurements^{18,19,20,21} of TRSB in [110] oriented tunnel junctions of YBCO. We

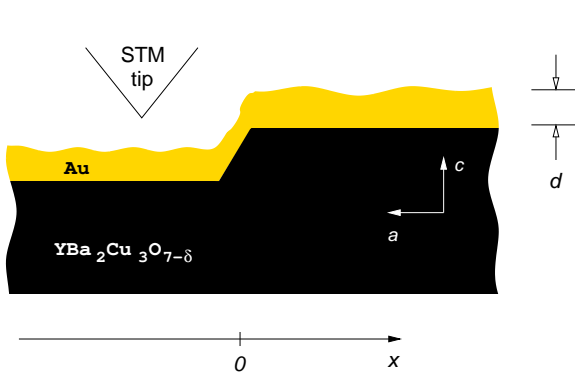


FIG. 1: We model the experimental setup by a half-infinite ($x \in [-\infty, 0]$) dirty normal metal in good contact with a [100] facet of rather clean YBCO ($x \in [0, \infty]$). The LDOS in the normal metal may be mapped out by STM.

note, however, that signatures of subdominant pairing is not always seen experimentally.^{22,23} In the N-side we include a pairing interaction that can be either attractive, repulsive, or zero. We assume that the gold metal is dirty, and include impurity scattering in the self-consistent t -matrix approximation,^{24,25} under the assumption that the impurities scatter isotropically (s -wave scattering only) in the Born limit. This corresponds to the Usadel approximation,²⁶ which is widely used to describe the proximity effect in contacts involving low- T_c superconductors. Since we are considering the high- T_c superconductors, which are clean materials with anisotropic pairing, we can not use Usadel's scheme; instead we solve the full Eilenberger equations^{27,28} for the quasiclassical Matsubara matrix Green's function $\hat{g}^M(\mathbf{p}_f, \mathbf{R}; \epsilon_n)$, where \mathbf{p}_f is the Fermi momentum, \mathbf{R} is the spatial coordinate, and $\epsilon_n = (2n + 1)\pi T$ (n integer) is the Fermion Matsubara frequency:

$$\begin{aligned} \left[i\epsilon_n \hat{\tau}_3 - \hat{\sigma}^M - \hat{\Delta}, \hat{g}^M \right] + i\mathbf{v}_f \cdot \nabla \hat{g}^M &= 0, \\ (\hat{g}^M)^2 &= -\pi^2. \end{aligned} \quad (1)$$

Here is $\hat{\tau}_3$ the third Pauli matrix in Nambu space, $\hat{\Delta}$ is the superconductor gap (pair potential), and $\hat{\sigma}^M$ is the sum of the impurity elastic and spin flip self energies $\hat{\sigma}^M = \hat{\sigma}_{imp}^M + \hat{\sigma}_{sf}^M$. We use units $\hbar = k_B = 1$, except in Table I.

The gap equation reads

$$\hat{\Delta}(\mathbf{p}_f, \mathbf{R}) = T \sum_{\epsilon_n}^{\epsilon_n < \omega_c} \int d\mathbf{p}'_f \lambda(\mathbf{p}_f, \mathbf{p}'_f, \mathbf{R}) \hat{f}^M(\mathbf{p}'_f, \mathbf{R}; \epsilon_n), \quad (2)$$

where \hat{f}^M is the off-diagonal part of the matrix Green's function \hat{g}^M , ω_c is an energy cut-off, and $\int d\mathbf{p}_f \dots$ denotes a Fermi surface average. In our model system, we assume that the interaction has a simple form

$$\lambda(\mathbf{p}_f, \mathbf{p}'_f, \mathbf{R}) = \begin{cases} \lambda_n, & \text{N side,} \\ \lambda_d \eta_d(\mathbf{p}_f) \eta_d(\mathbf{p}'_f) + \lambda_s, & \text{S side,} \end{cases} \quad (3)$$

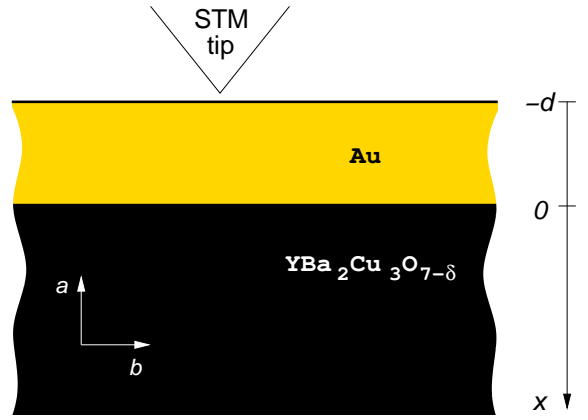


FIG. 2: The second model system is a more conventional proximity overlayer, where the LDOS at the normal metal surface may be probed by STM.

where λ_d and λ_s are the interaction strengths in the d -wave and s -wave channels, respectively, in the superconductor. The basis function in the d -wave channel is taken to have the form $\eta_d(\mathbf{p}_f) = \sqrt{2}(\hat{p}_x^2 - \hat{p}_y^2)$, $\int d\mathbf{p}_f \eta_d(\mathbf{p}_f) = 0$, $\int d\mathbf{p}_f |\eta_d(\mathbf{p}_f)|^2 = 1$. In the normal metal for attractive interaction $\lambda_n > 0$, while for repulsive interaction $\lambda_n < 0$. For attractive interaction, we can eliminate the cut-off ω_c and the interaction λ in favor of the bare bulk superconducting transition temperature T_c in the usual way,⁵ $\lambda^{-1} = \ln(T/T_c) + \sum_{n \geq 1} (n - 0.5)^{-1}$. For repulsive interaction, this procedure obviously fails, and we have a weak cut-off dependence. We take $\omega_c = 30T_c$, but we have checked that our results are not qualitatively changed for other values of ω_c .

With the pairing interaction in Eq. (3), the order parameter is

$$\Delta(\mathbf{p}_f, \mathbf{R}) = \begin{cases} \Delta_n, & \text{N side,} \\ \Delta_d \eta_d(\mathbf{p}_f) + \Delta_s, & \text{S side,} \end{cases} \quad (4)$$

where all amplitudes are in general complex quantities. We choose Δ_d real, while the phases of Δ_n and Δ_s relative to Δ_d are found self-consistently. We denote the maximum value of the d -wave component, $\max\{\Delta_d \eta_d(\mathbf{p}_f)\} = \sqrt{2}\Delta_d$, by Δ_0 .

The self energy from elastic impurity scattering has the form²⁵

$$\hat{\sigma}_{imp}^M(\mathbf{R}, \epsilon_n) = \frac{1}{2\pi\tau_{imp}} \int d\mathbf{p}_f \hat{g}^M(\mathbf{p}_f, \mathbf{R}; \epsilon_n), \quad (5)$$

and we shall use the mean free path $\ell = v_f \tau_{imp}$ as the input parameter, which takes the value $\ell_{n/s}$ in the N and S sides, respectively. We also include spin-flip scattering through the self energy²⁹

$$\hat{\sigma}_{sf}^M(\mathbf{R}, \epsilon_n) = \frac{1}{2\pi\tau_{sf}} \int d\mathbf{p}_f \hat{\tau}_3 \hat{g}^M(\mathbf{p}_f, \mathbf{R}; \epsilon_n) \hat{\tau}_3, \quad (6)$$

where the mean free path $\ell_{sf} = v_f \tau_{sf}$ is always assumed to be large compared to the elastic mean free path. The spin-flip process will ultimately set an upper limit on how long range the proximity effect is.⁷

The interface connecting the normal metal side and the superconductor side is described by Zaitsev's boundary condition,³⁰ valid for arbitrary transparency $\mathfrak{D}(\mathbf{p}_f)$. This model describes a wide specularly scattering contact with translational invariance along the interface. For simplicity we consider a two-dimensional system, with quasiparticles moving within the ab -plane in the superconductor which we also denote the xy -plane, with the x -axis extending perpendicular to the interface (as in Figs. 1-2) and the y -axis lies parallel to the interface. We assume circular Fermi surfaces in the two sides and take the angular dependence of the interface barrier as predicted by an interface δ -function potential of strength H_b , including the possibility of different Fermi velocities in the two sides (see e.g. Ref. 5). We assume that the effective masses in the two sides are the same (for a discussion of effective mass mismatch, see e.g. Ref. 31). For Zaitsev's boundary condition the momentum parallel to the interface is conserved, which means that the two different trajectory angles $\theta_{n/s}$ of the two sides, measured relative to the x -axis, are related as

$$v_{fs} \sin \theta_s = v_{fn} \sin \theta_n. \quad (7)$$

We assume that the Fermi velocity is larger in the normal metal than in the high- T_c superconductor, $0 < \alpha \equiv v_{fs}/v_{fn} \leq 1$. Quasiparticles travelling on trajectories with angles θ_n larger than a critical angle

$$\theta_c = \arcsin \alpha, \quad (8)$$

suffer total reflection. The interface transparency for angles $\theta_n < \theta_c$ is

$$\mathfrak{D}(\mathbf{p}_f) = \frac{4v_n v_s}{(v_n + v_s)^2 + 4H_b^2}, \quad (9)$$

where $v_{n/s} = v_{fn/s} \cos \theta_{n/s}$ are the projections on the interface normal of the Fermi velocities in the two sides. We use the model parameters α and $Z \equiv H_b/v_{fn}$ to parameterize the barrier transparency. The transparency for perpendicular incidence is denoted $\mathfrak{D}_0 = \alpha/[0.25(1 + \alpha)^2 + Z^2]$. We concentrate on the high-transparency limit, with values given in the experimental paper:¹⁰ $\mathfrak{D}_0 \sim 0.8 - 1.0$.

To compute the local density of states, we solve the retarded versions of the above equations, which are obtained by changing the superscript M to R and letting $i\epsilon_n \rightarrow \epsilon + i0^+$ in Eqs. (1) and (5)-(6). Here is $i0^+$ an infinitesimally small positive imaginary number. To speed up the convergence of the numerics we have kept this imaginary number finite equal to $i10^{-3}$. The gap profiles obtained within the Matsubara technique serve as input to the calculation of the retarded Green's functions. The

local density of states (LDOS) is defined as

$$\begin{aligned} \mathcal{N}(\mathbf{R}, \epsilon) &= \int d\mathbf{p}_f \mathcal{N}(\mathbf{p}_f, \mathbf{R}; \epsilon), \\ \mathcal{N}(\mathbf{p}_f, \mathbf{R}; \epsilon) &= -\frac{\mathcal{N}_f}{2\pi} \text{Im} \{ \text{Tr} [\hat{\tau}_3 \hat{g}^R(\mathbf{p}_f, \mathbf{R}; \epsilon)] \}, \end{aligned} \quad (10)$$

where \mathcal{N}_f is the density of states at the Fermi level in the normal state.

The above set of equations for the Green's functions and self-energies are solved self-consistently with numerical methods. This can be done quite efficiently with the Riccati parametrization technique.^{32,33,34,35}

III. RESULTS FOR THE NIS SYSTEM

Previously, Ohashi⁴¹ made a thorough investigation of the proximity effect in a clean system (mean free path $\ell \rightarrow \infty$) between a normal metal with attractive or repulsive s -wave interaction, in contact with a purely $d_{x^2-y^2}$ superconductor ($\lambda_s = 0$). See also the paper by Bruder.⁴² The central result of Ref. 41 is that for the [100] orientation an s -wave pair potential is induced in the N-side (for $\lambda_n \neq 0$), which also leads to spectral changes. For the [110] orientation the gap amplitude vanishes. The difference between the two orientations is easily understood by symmetry arguments: the positive and negative lobes of the $d_{x^2-y^2}$ order parameter contributes to the gap equation in the N-side with equal weights (but with opposite signs) in the [110] orientation and cancel exactly. This cancellation does not occur for the [100] orientation, and an s order parameter is induced. However, these results does not answer all question raised in the experiments.^{10,11} Also, the effects of impurities remain unclear. In the following we therefore present an extensive investigation of the proximity effect, including effects of impurity scattering and subdominant pairing in the S-side.

A. [100] orientation, $\lambda_n = 0$

In Fig. 3 we present a representative picture of the proximity effect at a [100] contact, in the absence of pairing interaction in N-side ($\lambda_n = 0$) but with a subdominant interaction channel in the S-side ($T_{cs} = 0.1T_c$). In part (a) we show the LDOS, and in (b) we show the order parameter profiles and some of the characteristic features in the LDOS. The parameters were chosen such that the elastic mean free path in the superconductor is $\ell_s = 25\xi_0$, corresponding to the typical low-temperature residual scattering rate $\tau \sim 1 - 10$ ps found in experiments.^{38,39} The normal metal side is assumed dirty, with $\ell_n = \xi_0 = v_f/T_c \sim 10 - 100$ nm typical for metals in general⁴⁰ and the Au overlayer in the experiment in particular.¹¹ Here we put $v_f \sim 10^6$ m/s in both sides, for simplicity. Note that the superconductor coherence length $\xi_\Delta = v_f/\pi\Delta_0 \lesssim \xi_0/2\pi$ is much smaller than

NM		
clean normal metal coherence length $\xi_{n0} = \frac{\hbar v_f}{2\pi k_B T}$	1 μm @ 1K	
normal metal elastic mean free path $\ell_n = v_f \tau$	10 – 100 nm	
dirty normal metal coherence length $\xi_n = \sqrt{\frac{\hbar D}{2\pi k_B T}}$	50 – 200 nm @ 1 K	
LTS		
YBCO		
superconductor gap size Δ_0	~ 1.5 meV [4]	20 – 25 meV [11,36]
superconductor coherence length $\xi_\Delta = \frac{\hbar v_f}{\pi \Delta_0}$	140 nm	16 \AA [37]
elastic mean free path $\ell_s = v_f \tau$	10 – 100 nm	250 – 2500 nm [38,39]
dirty superconductor coherence length $\xi_s = \sqrt{\frac{\hbar D}{2\Delta}}$	27-86 nm	not relevant ($\xi_\Delta \ll \ell_s$)

TABLE I: Order of magnitudes of some length scales relevant to the proximity effect in normal metals (NM), low- T_c superconductors (LTS), and YBCO. The diffusion constant is defined as $D = \frac{1}{3}v_f\ell$. For all estimates in NM and LTS we used $v_f \sim 10^6$ m/s [40]. The cited LTS gap value is for Nb [4]. The maximum d -wave gap amplitude is $\Delta_0 = \sqrt{2}\Delta_d$, and the magnitude given here is for the a -axis direction. The short coherence length in YBCO is usually estimated from the upper critical field in terms of Ginzburg-Landau theory³⁷ $H_{c2} = \Phi_0/2\pi\xi^2$, where $\Phi_0 = hc/2e$.

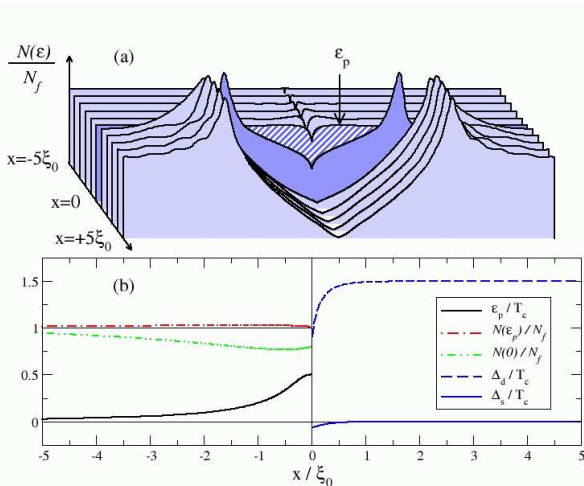


FIG. 3: The proximity effect at an [100] contact between a dirty normal metal ($\ell_n = \xi_0$) and a rather clean $d_{x^2-y^2}$ superconductor ($\ell_s = 25\xi_0$) with a subdominant s -wave component ($T_{cs} = 0.1T_c$). The pairing interaction in the normal metal side is $\lambda_n = 0$ (thus $\Delta_n = 0$). The temperature is $T = 0.05T_c$, and the spin flip mean free path is $\ell_{sf} = 100\xi_0$ in both sides. In (a) we show the density of states at $x = n\xi_0$ (integer $n = -5\dots 5$) for $\epsilon \in [-4T_c, 4T_c]$. There is a sudden change at $x = 0$ because of the interface backscattering for $\mathfrak{D}_0 = 0.9$ ($\alpha = 1$, $Z = 1/3$): the striped filled curve is at $x = 0^-$ and the dark filled is at $x = 0^+$. The density of states is normalized to N_f so that it approaches 1 for $\epsilon \gg T_c$. In (b) we show the spatial dependence of the peak $\epsilon_p(x)$ in the LDOS in the normal metal, the corresponding density of states $\mathcal{N}(\epsilon_p)$, the density of states at the Fermi level $\mathcal{N}(0)$, and the pair potentials Δ_d and Δ_s in the superconductor.

the length scale $\xi_0 = v_f/T_c$ we use. We summarize the relevant length scales found in real materials in Table I.

If the normal metal was clean, there would not be any signatures of the proximity effect in the LDOS⁴¹ (since the pair potential is zero for $\lambda_n = 0$). In contrast, in the

dirty case presented here we have clear signatures in the form of a pseudogap at low energies, that decays into the normal metal on the thermal coherence length scale $\xi_n = \sqrt{D/(2\pi T)}$, where $D = v_f\ell_n/3$ is the diffusion constant in the normal metal. To quantify the effect we show in Fig. 3(b) the spatial dependences of the pseudogap peak position $\epsilon_p(x)$ (solid black line), the LDOS at the peak position $\mathcal{N}(\epsilon_p)$ (red dashed-dotted line), and the LDOS at zero energy $\mathcal{N}(0)$ (green dashed-double-dotted line), where it is suppressed the most. The maximum deviation from the normal metal density of states is about 25%, which is much smaller than the 100% effect predicted in low- T_c s -wave superconductors^{1,2,3,6,7,8,9} at zero energy. This difference is due to the nodes in the $d_{x^2-y^2}$ -wave order parameter and the cancellation effects between the positive and negative lobes, which substantially reduce the influence of the unconventional superconductor on the LDOS in the normal metal.

The presence of a proximity effect at the junction signals a non-zero Fermi-surface average

$$\int d\mathbf{p}_f f^R(\mathbf{p}_f, \mathbf{R}; \epsilon) \neq 0 \quad (11)$$

in this region. This average is non-zero near the interface in both sides. Its non-zero value is intimately related to the suppression of the $d_{x^2-y^2}$ component.^{41,43,44} Since $f^R(\mathbf{p}_f, \mathbf{R}; \epsilon) \propto \eta_d(\mathbf{p}_f)$, a non-zero Fermi surface average can only be obtained for a spatially dependent $d_{x^2-y^2}$ -wave gap in a self-consistent solution where non-locality is taken into account. The average is also enhanced when the back-scattering probability at the interface $\mathfrak{R}_0 = 1 - \mathfrak{D}_0$ is non-zero, since then the importance of high angle trajectories $> \pi/4$ (for which the d -wave order parameter is negative) is reduced compared to the low angle trajectories $< \pi/4$ (for which the order parameter is positive).

In Fig. 3 we couple back the non-zero Fermi surface average of the off-diagonal Green's function in the superconductor side by having a small subdominant pair-

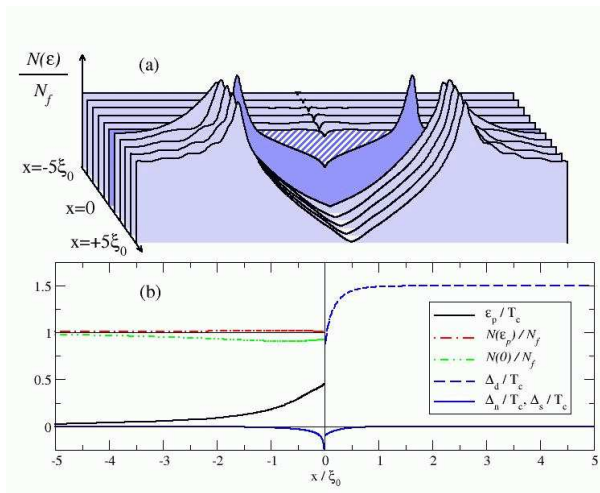


FIG. 4: The same as in Fig. 3, but with repulsive pairing interaction in the normal metal side $\lambda_n = -5$, which result in an induced pair-potential Δ_n in the normal metal.

ing interaction ($\lambda_s > 0$). We then obtain a non-zero subdominant order parameter component Δ_s near the interface in the superconductor. However, this component is always in phase with the dominant d -wave, and time-reversal symmetry is always conserved at the [100]-contact in the parameter space we have explored (mean free paths ranging from the clean limit $\ell_n \rightarrow \infty$ to the dirty limit $\ell_n \ll \xi_{n0}$ with a wide variety of barrier transparencies and subdominant pairing interactions). The effects of the s -wave gap on the local density of states is marginal.

B. [100] orientation, $\lambda_n < 0$

In Fig. 4 we present the proximity effect at a [100] contact, for the case of a repulsive pairing interaction in the N-side. We have in mind that the counter electrode in the experiment¹¹ was Au which is not a superconductor and might have a repulsive effective pairing interaction. The $d_{x^2-y^2}$ -wave pairing correlations leaks over to the N-side, which leads to the non-zero Fermi-surface average in Eq. (11). That average is coupled back through the repulsive pairing interaction λ_n , which leads to a non-zero pair potential Δ_n , that decays into the bulk normal metal. The subdominant component Δ_s on the S-side is not qualitatively affected by the induced pair potential on the N-side. The opposite is also true, the induced Δ_n is not qualitatively affected by the presence ($\lambda_s \neq 0$) or absence ($\lambda_s = 0$) of the component Δ_s . Thus, the proximity induced pair potential on the normal metal side is mainly due to the dominant $d_{x^2-y^2}$ component. We also note that the real combination $d + s$ is always favored in the system, as in the case $\lambda_n = 0$ above.

As for the LDOS, the induction of the gap amplitude Δ_n changes the density of states near the contact. There are new low-energy states, which are formed because of

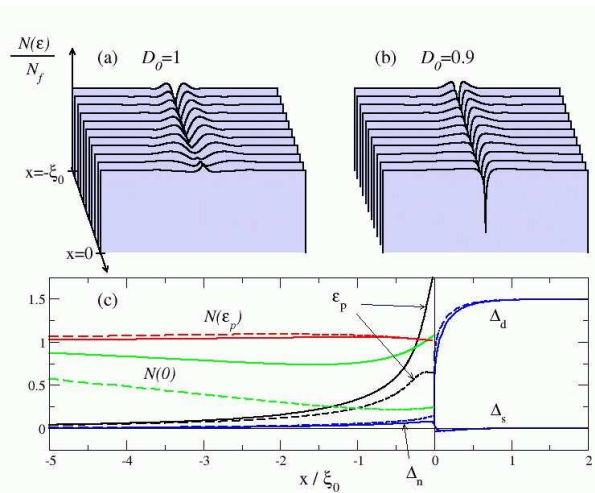


FIG. 5: Proximity effect at a [100] contact with a normal metal with attractive pairing interaction ($T_n = 0.01T_c < T = 0.05T_c$), for high barrier transparencies $\mathfrak{D}_0 = 1$ ($\alpha = 1, Z = 0$) in (a) and $\mathfrak{D}_0 = 0.9$ ($\alpha = 1, Z = 1/3$) in (b). All other model parameters are the same as in Figs. 3. Only the density of states in the normal metal at $x \in [-\xi_0, 0]$ (in steps of $0.1\xi_0$) for $\epsilon \in [-4T_c, 4T_c]$ is shown in (a)-(b). The solid (dashed) lines in (c) refer to the contact with $\mathfrak{D}_0 = 1$ ($\mathfrak{D}_0 = 0.9$).

the sign change of the order parameter field for quasiparticles travelling on low-angle trajectories $< \pi/4$ which connect the negative gap Δ_n on the N-side with the positive lobe of the $d_{x^2-y^2}$ order parameter on the S-side. This is analogous to the zero-energy bound states formed at a [110] surface of a $d_{x^2-y^2}$ superconductor,⁴⁵ and was also discussed in the study of the superclean case.⁴¹ In our case, the impurity scattering broadens the states considerably. Thus, compared with the case $\lambda_n = 0$ above, the LDOS peak position $\epsilon_p(x)$ is drawn closer to the Fermi surface. At the same time, the overall modulation of the LDOS in the normal metal is reduced compared to the case without the pairing interaction. Thus, contrary to our first expectations, an induced non-zero pair potential Δ_n in the normal metal reduces the proximity effect in the LDOS, as compared to the case $\Delta_n \equiv 0$. This is a unique feature of the dirty system.

C. [100] orientation, $\lambda_n > 0$

For the case of attractive interaction in the N-side, λ_n is positive which results in a sign change of the order parameter Δ_n compared to the repulsive interaction case considered above (see Fig. 5). At the same time the order parameter amplitude becomes larger and decays slower compared to the repulsive interaction case (analogous results were also found for the clean case in Ref. 41). As for the LDOS, the weight of the low-energy states is larger because of the larger pair potential, although the trajectories contributing to these states are at high angles $> \pi/4$. For a fully transparent interface,

the states are centered at zero energy, Fig. 5(a). For non-zero back-scattering at the junction, Fig. 5(b), the states are split, see Fig. 5(b), where the split size depends on the interface transparency ($\mathfrak{D}_0 = 0.9$ in the figure). The total effect of the proximity effect is enhanced for the case of attractive pairing interaction in the normal metal, compared to the case without interaction in Fig. 3. The LDOS variations can be as high as 80% for our choice of parameters, see Fig. 5(c).

Given the fact that there are low-energy states we are tempted to think that a TRSB combination $d_{x^2-y^2} + is$ could be formed (at least for $\mathfrak{D}_0 \equiv 1$ for which the split-effect is absent), instead of the real $d_{x^2-y^2} + s$ combination found above. If this was the case, the energy of the system might be lowered, similar to what happens at [110] surfaces or Josephson junctions.^{46,47,48,49} However, for the proximity contact we were never able to stabilize a TRSB state within the parameter space we have considered. We understand this result as due to a phase locking between the s -wave gaps in the N and S sides, to the dominant $d_{x^2-y^2}$, that prevents a relative phase $\pi/2$ between any two components to be formed. Compared to the Josephson junctions case, the two sides of the proximity contact are not independent: there is no bulk order parameter on the N-side that makes it possible to establish a phase difference $\pi/2$ over the junction. As for the subdominant s -wave order parameter on the S-side, it is due to the spatially varying $d_{x^2-y^2}$ order parameter, and is not induced by the bound state as in the [110] surface case. We also note that spontaneous symmetry breaking in the form of a paramagnetic instability^{34,48,50,51,52} is suppressed by impurity scattering and normal back-scattering at the junction.

D. [110] orientation

We now turn to the [110] orientation. In previous studies of the clean system,⁴¹ no gap amplitude was found in the normal metal side for reasons of symmetry. As for the LDOS in the N side, it is always unchanged in a clean system when the gap amplitude is zero. For $\lambda_n \equiv 0$, we find no signatures of the proximity effect in the LDOS in the dirty case either, which also follows from symmetry arguments. However, when we include a subdominant component in the superconductor side at a contact with [110] orientation, it will be formed $\pi/2$ out of phase with the dominant, and we have a TRSB state^{14,15} (this is opposite to the [100] case above). We note that some backscattering is necessary at the junction, i.e. if the transparency $\mathfrak{D}_0 \equiv 1$ there are no zero-energy states and no TRSB. As for the proximity effect in the N-side, high transparency is favorable. Thus, we concentrate on a window of intermediate transparencies, in order to establish a proximity effect between a TRSB $d_{x^2-y^2} + is$ state at a [110] interface to a normal metal, see Fig. 6. Clearly, the established is -part in the S-side, leads to a proximity induced is component also in the N-side that

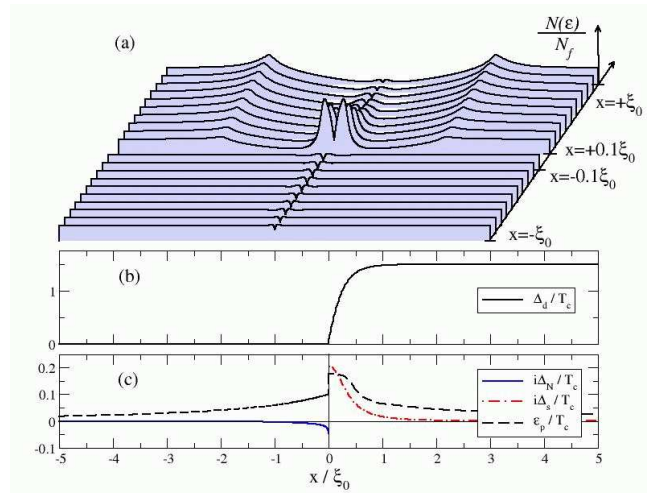


FIG. 6: The proximity effect at a [110] contact with $T_{cs} = 0.1T_c$. A subdominant component develops near the surface in the TRSB combination $d + is$ at the S-side. For intermediate transparencies, here $\mathfrak{D}_0 = 0.3$ ($\alpha = 1$, $Z^2 = 7/3$), the subdominant component induces an is -wave pair potential at the N-side ($\lambda_n = -5$). We have $T = 0.05T_c$, $\ell_n = \xi_0$, $\ell_s = 25\xi_0$, and $\ell_{sf} = 100\xi_0$.

decays into the bulk normal metal, although the effect is rather small and short range. The details of the window of transparencies depend on the mean free paths, as well as the interaction strengths. Typical values where there are TRSB and at the same time visible effects in the LDOS on the N-side are $\mathfrak{D}_0 \sim 0.1-0.5$, for our choice of parameters. The double peak structure on the S-side, see the (a)-part of the figure, decays on the coherence length scale, together with the subdominant component, red-dashed line in (c). Both this peak structure, and the peak structure in the LDOS at the N-side, [black dashed line in (c)], are related to, but not direct images of, the s -wave pair potentials $i\Delta_s$ and $i\Delta_n$ because of the importance of the impurity self-energy.

These results have the potential to serve as a probe of TRSB at [110] interfaces: as the temperature is decreased, the spectrum in the normal metal overlayer remains unchanged (equal to N_f for all energies) until the TRSB transition is reached, below which a small pseudo-gap develops as shown in Fig. 6. This probe is however not very quantitative and will not give direct information about the size of Δ_s , because of the masking effect of the impurity scattering. Rather, it would serve as a *yes/no* experiment, as to the existence or absence of TRSB at low temperatures.

The drawback of the above considerations is that they rely heavily on symmetry arguments. Thus, to a much higher degree than other results in this paper, non-specular interface scattering^{53,54,55,56,57,58} could be detrimental.

Another caveat is the possibility of d -wave pairing correlations (attractive or repulsive) in the normal metal. An induced d -wave pair potential leads to spectral

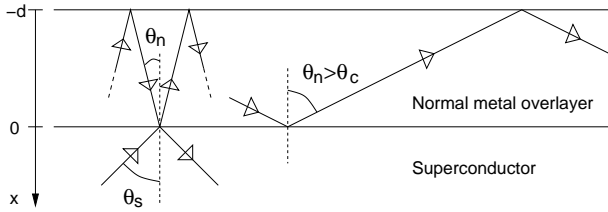


FIG. 7: Quasiparticles travelling on high-angle trajectories $\theta_n > \theta_c$ suffer total reflection at the NIS interface because of the Fermi velocity mismatch $v_{fn} > v_{fs}$ (the trajectory to the right). On other trajectories $\theta_n < \theta_c$, quasiparticles are partially reflected in accordance with Eq. (9).

changes in the normal metal for the [110] orientation also in the absence of TRSB, thereby spoiling the symmetry argument. The LDOS is enhanced at low energy by the formation of low-energy Andreev states broadened by impurity scattering, if the d -wave pairing correlations are oriented as [110] relative to the interface. This is similar to what happens at Josephson junctions between two d -wave superconductors.¹⁷ However, it seems unlikely that spatially homogeneous d -wave pairing correlations with a well-defined orientation relative to the interface could exist in a normal metal such as Au.

However, these complications are temperature-independent and should not appear suddenly at the low-temperature TRSB transition. Thus, a smooth but rather sudden change in the normal metal spectrum near the interface as a function of temperature can be a signal of TRSB.

IV. RESULTS FOR THE INIS SYSTEM

Let us now study the change in the density of states in a normal metal overlayer in good contact with a [100] facet, see Fig. 2. Because of the absence of a bulk boundary condition in the normal metal overlayer, we solve Eq. (1) iteratively until self-consistency is reached in the overlayer, under the assumption of specular reflection at the vacuum-normal metal surface (at $x = -d$). Including the possibility of a Fermi velocity mismatch, we have two types of trajectories when we solve Eq. (1) depending on if the trajectory angle θ_n is larger or smaller than the critical angle for total inner reflection in Eq. (8). We show the trajectories in Fig. 7. Note that when we draw the trajectories in Fig. 7 we do not imply that quasiparticles move ballistically. Rather, the lines denote trajectories along which we solve Eq. (1). Quasiparticles diffuse, which is described by solving the impurity self-energies in Eqs.(5)-(6) self-consistently with the Green's function in Eq. (1).

Because of the severe isotropization effect caused by impurity scattering, we do not expect non-specular scattering to drastically alter our results. In fact, similar results for the LDOS in the superconductor as we find was already reported by Golubov and Kupriyanov.^{43,44}

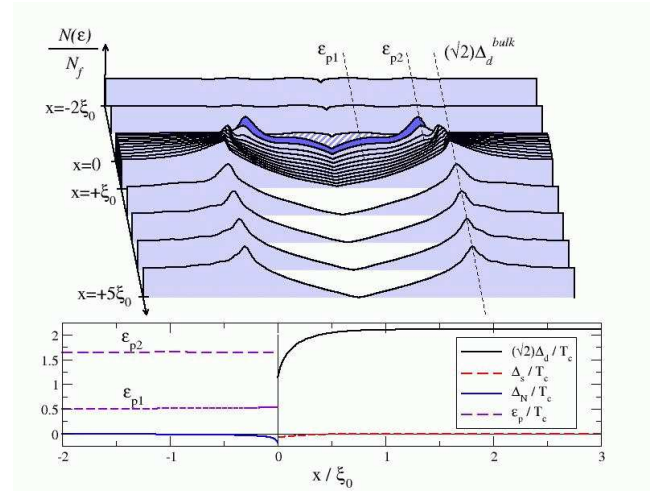


FIG. 8: The proximity effect at a [100] facet with a $d = 2\xi_0$ thick normal metal overlayer. We have $T = 0.05T_c$, $T_{cs} = 0.1T_c$, $\lambda_n = -5$, $\ell_n = v_{fn}/T_c = 2v_{fs}/T_c = 2\xi_0$, $\ell_s = 25\xi_0$. The Fermi velocity mismatch is $v_{fn} = 2v_{fs}$ ($Z = 0$), which leads to $\mathcal{D}(\theta_n = 0) \approx 0.9$ and $\theta_c \approx 30^\circ$.

They used the dirty normal metal overlayer as a model for a diffusive boundary condition for the superconductor. In their case, however, the dirty layer thickness was assumed small, $d \ll \sqrt{\xi_0 \ell_n}$. Here we relax this assumption and study in more details the effect of the superconductor in the normal metal.

We present typical results for the order parameters and the LDOS for a [100] contact in Fig. 8. We find that the LDOS is almost independent of coordinates in the normal metal, but depends on the thickness of the overlayer. There are quasibound states, seen as peaks in the LDOS, reflecting interference between electrons and holes in the dirty normal metal in contact with the superconductor.¹⁷ The energies of these states depends on the thickness of the overlayer. In a normal metal in good contact with an s -wave superconductor, there is a minigap E_g of the order of the Thouless energy $E_{th} = D/d^2$ ($D = \frac{1}{3}v_f\ell$), below which the density of states vanish (for a discussion see e.g. Ref. 8 and references therein). Because of the nodes of the $d_{x^2-y^2}$ order parameter and impurity scattering, this effect is removed and only a suppression of the low-energy density of states remains. As in the NIS case discussed in the previous section, the LDOS in the normal metal mainly reflects the influence of the impurity self-energy and does not contain direct information about the induced pair potential Δ_n for non-vanishing interaction $\lambda_n \neq 0$.

In Fig. 9 we show typical results for the [110] contact. The peaks in the LDOS in the overlayer are shifted,¹⁷ as compared with the [100] contact. This reflects the formation of the zero-energy states.^{17,45} For lower transparencies, the TRSB state can be favorable, which leads to a split of the zero-energy peak, similar to the situation in Fig. 6.

In Fig. 10 we plot the surface LDOS and the conduc-

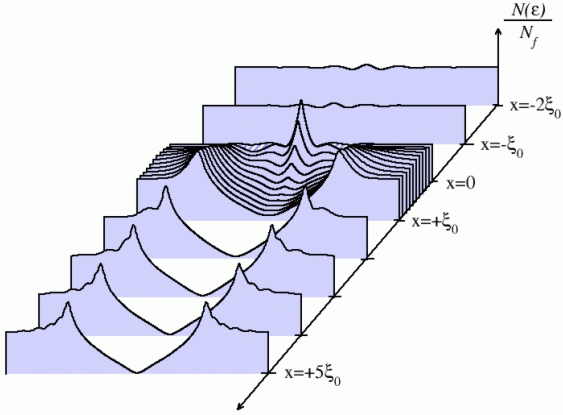


FIG. 9: The same as in Fig. 8, but for the [110] orientation. For these model parameters only a d -wave order parameter exist. The peak positions in the normal metal are at $\epsilon_p = \{0, 0.96T_c, 1.98T_c\}$.

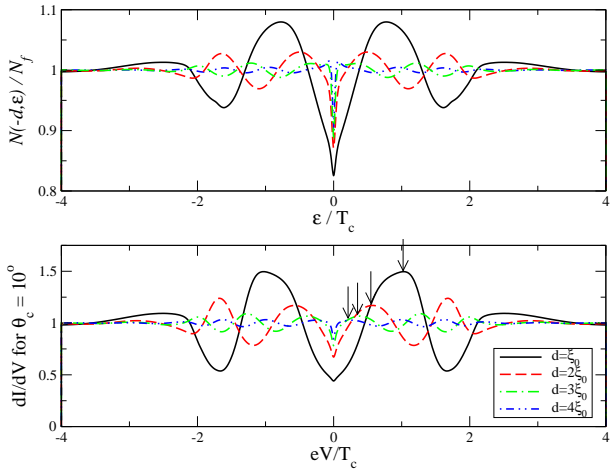


FIG. 10: (a) The surface local density of states and (b) the conductance as it would be measured by STM according to Eq. (12) for a $\theta_c^{tip} = 10^\circ$ wide tunnel cone, for several different thicknesses of the normal metal overlayer ranging from $d = \xi_0$ to $d = 4\xi_0$. The mean free path is $\ell_n = 2\xi_0$ and total isotropization by the impurities has not yet occurred which leads to an enhancement of the modulation in the surface density of states as seen in the STM conductance [note the different scales in (a) and (b)]. The arrows indicate how the peak positions move toward the Fermi level for increased overlayer thickness. The other model parameters are the same as in Fig. 8. Note that the red dashed curves corresponds to the data in Fig. 8.

tance at the [100] contact as it would be measured by an STM tip, as a function of layer thickness. For simplicity we model the tunnel barrier between the tip and the overlayer by a tunnel cone of width $2\theta_{cone}^{tip}$, with transparency \mathcal{D}_0^{tip} for angles within the cone and transparency 0 for angles outside. The conductance is related to the angle

resolved surface local density of states $\mathcal{N}(x = -d, \theta_n; \epsilon)$ as

$$\frac{dI}{dV}(V) = \frac{1}{R_n^{tip}} \int_{-\theta_c^{tip}}^{\theta_c^{tip}} d\theta_n \mathcal{D}_0^{tip} \frac{\mathcal{N}(-d, \theta_n; eV)}{N_f}, \quad (12)$$

where R_n^{tip} is the resistance of the tip-sample contact in the normal state (we normalize $\int d\theta_n \mathcal{D}_0^{tip}(\theta_n) = 1$). For intermediate overlayer thicknesses, total isotropisation of the LDOS by the impurities might not have occurred, and a small tunnel cone can enhance the structures in the LDOS as seen by the STM, since trajectories close to the interface normal is selected.

V. SUMMARY AND CONCLUSIONS

We have studied the proximity effect in good contacts between $d_{x^2-y^2}$ superconductors and normal metals. We have investigated the effects of impurity scattering, a subdominant component of s -wave symmetry in the superconductor side, and a proximity induced order parameter in the N side. For the [100] orientation, we always find a real combination $d_{x^2-y^2} + s$ in the superconductor. At the same time, the N side gap amplitude is phase locked to the d -wave order parameter on the S-side. On the other hand, for a [110] contact with intermediate values of the transparency, a TRSB $d_{x^2-y^2} + is$ order parameter on the S side, induces an is gap amplitude also on the N side. We note that the subdominant is component in the S side is not due to the proximity effect; rather, it is due to the formation of the bound state at the [110] interface in the usual way.^{14,15} The signatures of the proximity effect at [110] contacts could serve as fingerprints of TRSB, with the caveat of possible breaking of the “selection rule” by e.g. non-specular scattering or d -wave pairing correlations in the normal metal.

We finish with a comparison with the experiments.^{10,11} We can not find evidence of the unusual symmetry breaking proximity effect at [100] contacts that was proposed in Ref. 10. The proximity induced pair potential in the normal metal is due to the suppression of the d -wave order parameter and no non-trivial relative phase develops. However, a serious comparison with the experiment of Kohen *et al.*¹⁰ can not be done since that was a transport experiment where the conductance was measured. At the same time, the analysis¹⁰ in terms of a BTK-type theory with postulated pair potentials and no considerations of real non-equilibrium effects, rather than self-consistently computed quantities, might be too simplistic. Especially when the contact has high transparency. For example, a dirty normal metal (instead of a clean metal as in the BTK theory) in contact with a d -wave superconductor can lead to quite different results for the conductance, as shown theoretically recently.^{59,60} Those considerations were limited to point contacts with the superconductor a purely d -wave ($\lambda_s = 0$), super-clean ($\ell_s \rightarrow \infty$), unperturbed reservoir.

On the other hand, our results is in *qualitative* agreement with the experimental results of Sharoni *et al.*¹¹ The modulations of the density of states consists of a suppression of the density of states at the Fermi level (but not to zero), with a quite well defined peak position ϵ_p . These structures decay into the normal metal on the scale ξ_n . However, an *unambiguous quantitative* fit between theory and data is hard to make for several reasons. On the theory side, even within our simple model, the local density of states is sensitive to many parameters, such as the mean free paths, the interface resistance, the Fermi velocities, as well as pairing interaction strengths. The choice of parameters is not unique. On the experimental side, only a limited number of spectra were shown, although many points $\epsilon_p(x)$ were reported. In particular, the spectra for small distances were not shown, for which ϵ_p were reported to be spectacularly large ~ 15 meV $\sim 0.75\Delta_0$, which is hard to reproduce in theory ($\epsilon_p \sim 0.25\Delta_0$ in Figs. 3-6). We note, however, that similar (but not as large) discrepancies between theory and experiments were recently reported⁴ also for low- T_c contacts (Nb-Au). Although in that case, the discrepancy was the largest for large distances. Another problem is that the modulation in the LDOS appears to be larger than we find (unless the effective pairing interaction in Au is attractive which seems unlikely). In particular $\mathcal{N}(\epsilon = 0)$ is suppressed more than we find for

the NIS system. On the other hand, the experimental situation was not clean cut: a mixture of the NIS and INIS systems appears to be relevant. For large (small) distances from the a -facet, the setup appears to be NIS-like (INIS-like). It is also unclear where along the x -axis in our Fig. 1 the spectra were actually recorded. From their Figs. 1-2 it appears that the spectra were actually taken at points corresponding to $x > 0$ in our Fig. 1, i.e. into the YBCO c -axis.

Despite these complications, it is quite plausible that the experimental results could be explained by the more conventional type of proximity effect we have discussed in this paper, rather than an exotic proximity effect that involves symmetry breaking.

Acknowledgments

I would like to thank J.A. Sauls for encouragements to finish this work, and for pointing out the potential importance of repulsive d -wave pairing correlations in the normal metal. Financial support was provided by the Swedish Foundation for International Cooperation in Research and Higher Education (STINT) and the Wenner-Gren foundations.

-
- ¹ G. Deutscher and P. G. de Gennes, in *Superconductivity*, edited by R. D. Parks (Marcel Dekker, Inc., New York, 1969), vol. 2, p. 1005.
- ² S. Gueron, H. Pothier, N. O. Birge, D. Esteve, and M. H. Devoret, *Phys. Rev. Lett.* **77**, 3025 (1996).
- ³ N. Moussy, H. Courtois, and B. Pannetier, *Europhys. Lett.* **55**, 861 (2001).
- ⁴ A. K. Gupta, L. Créteinon, N. Moussy, B. Pannetier, and H. Courtois, *Phys. Rev. B* **69**, 104514 (2004).
- ⁵ G. Kieselmann, *Phys. Rev. B* **35**, 6762 (1987).
- ⁶ A. A. Golubov and M. Y. Kupriyanov, *J. Low Temp. Phys.* **70**, 83 (1988).
- ⁷ W. Belzig, C. Bruder, and G. Schön, *Phys. Rev. B* **54**, 9443 (1996).
- ⁸ S. Pilgram, W. Belzig, and C. Bruder, *Phys. Rev. B* **62**, 12462 (2000).
- ⁹ W. Belzig, F. K. Wilhelm, C. Bruder, G. Schön, and A. Zaikin, *Superl. Microstr.* **25**, 1251 (1999).
- ¹⁰ A. Kohen, G. Leibovitch, and G. Deutscher, *Phys. Rev. Lett.* **90**, 207005 (2003).
- ¹¹ A. Sharoni, I. Asulin, G. Koren, and O. Millo, *Phys. Rev. Lett.* **92**, 017003 (2004).
- ¹² G. E. Blonder, M. Tinkham, and T. M. Klapwijk, *Phys. Rev. B* **25**, 4515 (1982).
- ¹³ Y. Tanaka and S. Kashiwaya, *Phys. Rev. Lett.* **74**, 3451 (1995).
- ¹⁴ M. Matsumoto and H. Shiba, *J. Phys. Soc. Jpn.* **64**, 3384 (1995).
- ¹⁵ M. Fogelström, D. Rainer, and J. A. Sauls, *Phys. Rev. Lett.* **79**, 281 (1997).
- ¹⁶ S. Kashiwaya and Y. Tanaka, *Rep. Prog. Phys.* **63**, 1641 (2000).
- ¹⁷ T. Löfwander, V. S. Shumeiko, and G. Wendin, *Supercond. Sci. Technol.* **14**, R53 (2001).
- ¹⁸ M. Covington, M. Aprili, E. Paraoanu, L. H. Greene, F. Xu, J. Zhu, and C. A. Mirkin, *Phys. Rev. Lett.* **79**, 277 (1997).
- ¹⁹ L. H. Greene, M. Covington, M. Aprili, E. Badica, and D. E. Pugel, *Physica B* **280**, 159 (2000).
- ²⁰ R. Krupke and G. Deutscher, *Phys. Rev. Lett.* **83**, 4634 (1999).
- ²¹ A. Sharoni, O. Millo, A. Kohen, Y. Dagan, R. Beck, G. Deutscher, and G. Koren, *Phys. Rev. B* **65**, 134526 (2002).
- ²² L. Alff, H. Takashima, S. Kashiwaya, N. Terada, H. Ihara, Y. Tanaka, M. Koyanagi, and K. Kajimura, *Phys. Rev. B* **55**, R14757 (1997).
- ²³ N.-C. Yeh, C.-T. Chen, G. Hammerl, J. Mannhart, A. Schmehl, Schneider, R. R. Schulz, S. Tajima, K. Yoshida, D. Garrigus, et al., *Phys. Rev. Lett.* **87**, 087003 (2001).
- ²⁴ D. Xu, S.-K. Yip, and J. A. Sauls, *Phys. Rev. B* **51**, 16233 (1995).
- ²⁵ A. A. Abrikosov, L. P. Gorkov, and I. E. Dzyaloshinski, *Methods of Quantum Field Theory in Statistical Physics* (Dover Publications, Inc., New York, 1975).
- ²⁶ K. D. Usadel, *Phys. Rev. Lett.* **25**, 507 (1970).
- ²⁷ G. Eilenberger, *Z. Phys.* **214**, 195 (1968).
- ²⁸ J. W. Serene and D. Rainer, *Phys. Rep.* **101**, 221 (1983).
- ²⁹ J. Rammer and H. Smith, *Rev. Mod. Phys.* **58**, 323 (1986).

- ³⁰ A. V. Zaitsev, Zh. Eksp. Teor. Fiz **86**, 1742 (1984), [English translation Sov. Phys. JETP **59**, 1015 (1985)].
- ³¹ B. Ashauer, G. Kieselmann, and D. Rainer, J. Low Temp. Phys. **63**, 349 (1986).
- ³² Y. Nagato, K. Nagai, and J. Hara, J. Low Temp. Phys. **93**, 33 (1993).
- ³³ N. Schopohl and K. Maki, Physica B **204**, 214 (1995).
- ³⁴ A. Shelankov and M. Ozana, Phys. Rev. B **61**, 7077 (2000).
- ³⁵ M. Eschrig, Phys. Rev. B **61**, 9061 (2000).
- ³⁶ A. Damascelli, Z. Hussain, and Z.-X. Shen, Rev. Mod. Phys. **75**, 473 (2003).
- ³⁷ D. N. Zheng, A. M. Campbell, J. D. Johnson, J. R. Cooper, F. J. Blunt, A. Porch, and P. A. Freeman, Phys. Rev. B **49**, 1417 (1994).
- ³⁸ D. A. Bonn, S. Kamal, K. Zhang, R. Liang, D. J. Baar, E. Klein, and W. N. Hardy, Phys. Rev. B **50**, 4051 (1994).
- ³⁹ D. Duffy, P. J. Hirschfeld, and D. J. Scalapino, Phys. Rev. B **64**, 224522 (2001).
- ⁴⁰ N. W. Ashcroft and N. D. Mermin, *Solid State Physics* (Saunders College Publishing, 1976).
- ⁴¹ Y. Ohashi, J. Phys. Soc. Jpn. **65**, 823 (1996).
- ⁴² C. Bruder, Phys. Rev. B **41**, 4017 (1990).
- ⁴³ A. A. Golubov and M. Y. Kupriyanov, JETP Letters **67**, 501 (1998).
- ⁴⁴ A. A. Golubov and M. Y. Kupriyanov, Superlattices and Microstructures **25**, 949 (1999).
- ⁴⁵ C.-R. Hu, Phys. Rev. Lett. **72**, 1526 (1994).
- ⁴⁶ M. Sigrist, Prog. Theor. Phys. **99**, 899 (1998).
- ⁴⁷ M. Fogelström and S.-K. Yip, Phys. Rev. B **57**, R14060 (1998).
- ⁴⁸ T. Löfwander, V. S. Shumeiko, and G. Wendin, Phys. Rev. B **62**, R14653 (2000).
- ⁴⁹ M. H. S. Amin, A. N. Omelyanchouk, and A. M. Zagorskin, Phys. Rev. B **63**, 212502 (2001).
- ⁵⁰ S. Higashitani, J. Phys. Soc. Jpn. **66**, 2556 (1997).
- ⁵¹ A. L. Fauchere, W. Belzig, and G. Blatter, Phys. Rev. Lett. **82**, 3336 (1999).
- ⁵² Y. S. Barash, M. S. Kalenkov, and J. Kurkijärvi, Phys. Rev. B **62**, 6665 (2000).
- ⁵³ M. Matsumoto and H. Shiba, J. Phys. Soc. Jpn. **64**, 1703 (1995).
- ⁵⁴ Y. S. Barash, A. A. Svidzinsky, and H. Burkhardt, Phys. Rev. B **55**, 15282 (1997).
- ⁵⁵ T. Lück, U. Eckern, and A. Shelankov, Phys. Rev. B **63**, 064510 (2001).
- ⁵⁶ Y. Asano, Phys. Rev. B **64**, 014511 (2001).
- ⁵⁷ Y. Asano and Y. Tanaka, Phys. Rev. B **65**, 064522 (2002).
- ⁵⁸ Y. Nagato and K. Nagai, Phys. Rev. B **69**, 104507 (2004).
- ⁵⁹ Y. Tanaka, Y. V. Nazarov, and S. Kashiwaya, Phys. Rev. Lett. **90**, 167003 (2003).
- ⁶⁰ Y. Tanaka, Y. V. Nazarov, A. A. Golubov, and S. Kashiwaya, Phys. Rev. B **69**, 144519 (2004).